# Digital Mirror Devices for Mode Selective Excitation in Multimode Fibers

Andreas Ahrens, Steffen Lochmann and Peter Bartmann
*Hochschule Wismar, University of Technology, Business and Design, Philipp-Müller-Straße 14, 23966 Wismar, Germany*

Keywords: Optical MIMO, Space Division Multiplexing, Digital Mirror Devices (DMDs), Digital Light Processor (DLP), Mode Combining.

Abstract: Space division multiplex (SDM) in optical communications became an attractive research topic in recent years. A tremendous increase of data rates was exposed. In optical multiple-input multiple-output (OMIMO) SDM can be achieved by using separated fiber cores or several modes in multimode fibers (MMF). This paper tackles the task of mode selective excitation in MMFs. A completely new approach is shown utilizing digital mirror devices (DMDs) in this field. However, finding the optimal coupling conditions is a complex task due to the blazed grated structure of the micromirror array (MMA). A possible and intuitive solution for that problem is shown. Still, the benefits of such DMDs lies in the flexibility of mode excitation and the low insertion loss of around $-1.27$dB. This paper shows that the mode separation is comparative to mode excitation achieved with offset splices.

## 1 INTRODUCTION

Time division, wavelength and polarization multiplexing as well as high order modulation schemes have been developed coping with the exponential grow of data traffic in optical networks and have reached a state of maturity. Therefore, there exists an increasing interest in optical space division multiplexing (SDM). Adapting well-known wireless communications multiple-input multiple-output (MIMO) techniques to optical multiple-input multiple-output (OMIMO) transmission has been discussed in several papers like (Hsu et al., 2004; Hsu et al., 2006). In analogy to wireless communications, where spatial diversity gained by separated antennas is sufficient for a MIMO channel, OMIMO exploits mode diversity in multimode fibers (MMFs) among others. However, the first experiment for modal multiplexing dates back to 1982, where it was demonstrated in a 10-m long MMF (Berdagué and Facq, 1982). Newer publications show the feasibility of $2 \times 2$ up to $12 \times 12$ OMIMO systems in longer optical links of km-domain (Shah et al., 2005; Ryf et al., 2012). However, efficient excitation of specific modes in a MMF and their respective coupling and splitting is an open question.

This paper tackles the problem of mode selective excitation into conventional MMFs. Conventional approaches use centric and eccentric splices of a singlemode fiber (SMF) to a MMF (Schollmann et al., 2008). Due to the offset launching condition different modegroups are excited within the MMF depending on the eccentricity of the splice. Afterwards two or more modegroups in different MMFs are combined using fusion couplers. The hard reproducibility as well as the low flexibility are two drawbacks of this method. Another approach is to utilize spatial light modulators (SLMs). With SLMs as described in (Gu et al., 2013), for instance, individual modes can be excited with high contrast. Nevertheless, the attenuation due to the serial mode combining with semipermeable mirror couplers, which has to be used for a concatenation of SLMs, leads to an exponential growing power loss of 3dB in each step.

Addressing these problems this paper shows a new approach utilizing Digital Light Processor® (DLP) chips as coupling devices. The use of digital mirror devices (DMDs) in optical networks is described for one source in (Yoder et al., 2001), where the DMD has been used as a signal level controlling or network switching device. However, this paper extends its usability for SDM. The micromirror array (MMA) of a DMD has to be considered as a diffraction grating with blazed condition. Hence, the reflection of an inciting laser beam produces multiple diffraction maximums. Finding the global maximum in a mechanical



Ahrens, A., Lochmann, S. and Bartmann, P.
Digital Mirror Devices for Mode Selective Excitation in Multimode Fibers.
DOI: 10.5220/0005948500190024
In *Proceedings of the 13th International Joint Conference on e-Business and Telecommunications (ICETE 2016) - Volume 3: OPTICS*, pages 19-24
ISBN: 978-989-758-196-0

setup becomes a complex task. To avoid possible side effects of this in the OMIMO field new technology this paper concentrates on $2 \times 2$ OMIMO. This contribution is structured as follows: Sec. II starts with a short description of the coupling system. More in detail Sec. III defines parameters as well as the coordinate systems used to determine the diffraction behaviour of the DLP in Sec. IV. The mathematical description is then used in Sec. V finding optimal coupling conditions for the experimental setup. Sec. VI shows how the theory is realized and the first results achieved with visible light. They are compared to previous results from (Sandmann et al., 2014). The paper closes with a conclusion-section in VII.

## 2 UTILIZING DMDS IN OPTICAL MIMO

The breakthrough of the DLP technology can be traced back to efforts made by Texas Instruments (TI) at the beginning of the eighties, more precisely to Larry J. Hornbeck. The heart of a DLP projector is the DMD, which is patented by TI in 1986. The DMD consists of thousand of small mirrors having sizes in micrometer domain. The micromirrors are synonymously referred as pixels. The principle of a DMD is quite simple: each mirror can be tilted such that a light source is reflected to either an optical output system or an absorber. Hence, each pixel can be switched into so called 'on'- and 'off'-states. This principle is adapted for OMIMO as depicted in Fig. 1.

Fig. 1 shows the principle for the coupling process. Utilizing the property that each single mirror can be addressed to two opposite states, two independent sources can be arranged in front of the DLP

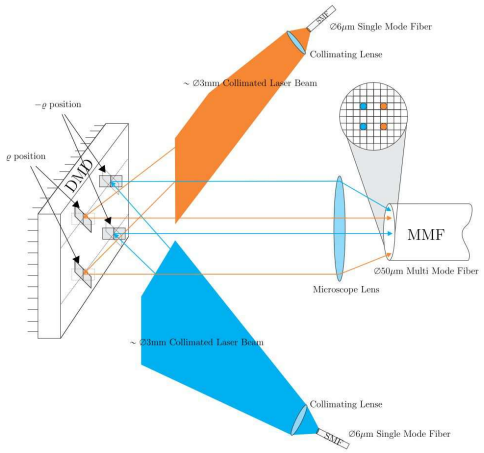


Figure 1: DMD supported optical space division multiplexing.

such that the main output direction of both reflected laser beam patterns is equal for both sources. The light sources are simply two SMF at which ends are collimating lenses to widen the light into collimated laser beams. These beams are reflected by the MMA where mirrors in 'on'-state reflect only one source to the output direction, for the other source mirrors in 'off'-state do. In this output direction an optic focuses the reflected laser beams onto a MMF. Thus, the tilt pattern on the MMA performs SDM. A flexible solution for a parallel excitation of low and high order modes can be designed.

## 3 DEFINITIONS

This section defines in a first step two different coordinate systems: one aligned with the DLP, the other one with the setup as well as their mathematical connectedness. In a second step the coupling parameters are defined in the second space.

The whole mathematical description is made in the direction cosine space (DCS) (Tang, 2007) whose axes are orientated with the micromirror vertices. Fig. 2 illustrates its orientation. The origin lies in the MMAs center. The tilt axes of each micromirror is parallel to $\alpha = -\beta$. This means in other words that the normal of each mirror lies parallel to the plane spanned by the $\gamma$-axis and the line $\alpha = \beta$. In the 'on'- or 'off'-state of a pixel the angle between the normal of the mirror and the $\gamma$-axis is either $+\rho$ or $-\rho$, respectively.

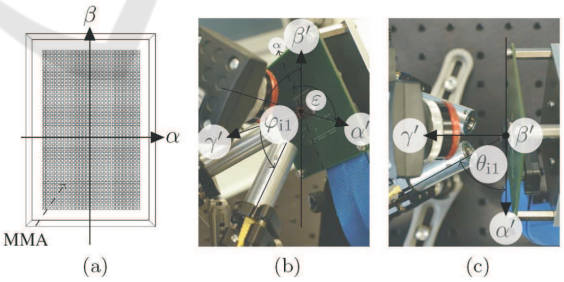


Figure 2: Experimental setup and its coordinates of the direction cosine space.

The second DCS is motivated by the aim that the experimental setup is symmetric related to the vertical plane on an optical breadboard. Considering that it is defined as depicted in Fig. 2 b) and 2 c). The DMD is rotated in the $\alpha'\beta'$-plane by $\varepsilon$ such each normal of a micromirror is parallel to the $\alpha'\gamma'$-plane independent on the state of the mirror. Hence, mirrors in 'on'-state can be used by one source, mirrors in 'off'-state by

the other source. The two DCSs are connected by

$$\begin{pmatrix} \alpha' \\ \beta' \end{pmatrix} = \mathbf{R} \begin{pmatrix} \alpha \\ \beta \end{pmatrix} \tag{1}$$

and

$$\gamma' = \gamma, \tag{2}$$

where **R** is a simple two dimensional rotation matrix.

There are two coupling parameters for each direction defined, where Fig. 2 exemplary shows them for the first input direction. The angle between the projection of the location vector of a source onto the $\alpha'\gamma'$-plane and the $\gamma'$-axis is called $\theta$ and the angle between the location vector and the $\beta'$-axis is $\varphi$. The two angles are orthogonal to each other. Subscripts like i1, i2 and o denotes the connection of an parameter to the first or second input or the output direction. By applying simple vector calculation as well as the connection between a Cartesian space and the DCS one can easily derive the association between coupling parameters and the DCS.

$$\alpha' = \cos(\theta)\sin(\varphi) \tag{3}$$

$$\beta' = \cos(\varphi) \tag{4}$$

## 4 DIFFRACTION BEHAVIOUR OF THE MMA

Due to the physical structure of the MMA, the DMD has to be considered as a two dimensional blazed grating. If the mirrors are not tilted, the MMA reacts as a common diffraction grating with the difference that the light is reflected instead of passing a two dimensional lattice. In the case of one dimension the macroscopic equation of diffraction is given by

$$\sin\xi_i \pm \sin\xi_o = m\frac{\lambda}{g}, \tag{5}$$

where $\xi_\mathrm{i}$ is the incident angle, $\xi_\mathrm{o}$ the output angle, $\lambda$ the used wavelength and $g$ the grating constant (Goodman, 2005). Note that the angles $\xi$ are measured to the array normal, which is different to the definition of $\theta$. The variable $m$ gives the order of the grating which is an integer limited by physical possible directions. In the setup corresponding angles of zeroth order are given by

$$\theta_\mathrm{o} = \pi - \theta_\mathrm{i} \tag{6}$$

and

$$\varphi_\mathrm{o} = \pi - \varphi_\mathrm{i}\,. \tag{7}$$

In (Harvey and Vernold, 1998) the derivation of (5) to the appropriate DCS representation is presented. By extending these equations to the two dimensional case the grating behaviour can be described by

$$\alpha_\mathrm{o} + \alpha_\mathrm{i} = \left(m\frac{\lambda}{g}\right) \tag{8}$$

and

$$\beta_\mathrm{o} + \beta_\mathrm{i} = \left(n\frac{\lambda}{g}\right)\,. \tag{9}$$

The transition from the macroscopic equation to the real intensity distribution of the reflected light has to be taken in order to find optimal coupling parameters. By neglecting the faceted profile of the MMA (Hayat, ), i.e., the blazed structure, and by utilizing the same mathematical tools as in (Harvey and Vernold, 1998), the full intensity distribution is defined by

$$I_\mathrm{D}(\alpha,\beta) = I_0 \left(\frac{\sin\left(P_\alpha \pi (g/\lambda)\,(\alpha-\alpha_\mathrm{o})\right)}{P_\alpha \sin\left(\pi (g/\lambda)\,(\alpha-\alpha_\mathrm{o})\right)}\right)^2 \left(\frac{\sin\left(P_\beta \pi (g/\lambda)\,(\beta-\beta_\mathrm{o})\right)}{P_\beta \sin\left(\pi (g/\lambda)\,(\beta-\beta_\mathrm{o})\right)}\right)^2 . \tag{10}$$

The number of micromirrors (pixels) in $\alpha$- and $\beta$-direction is denoted by $P_\alpha$ and $P_\beta$. Under the condition that (8) and (9) hold, (10) becomes the normalization constant $I_0$ which is a multiple occurred global maximum.

By considering the profile of the MMA one takes the step into the blazed grated structure. Due to the symmetric setup the blazed behaviour influences the output parameter $\theta_\mathrm{o}$ whereas the $\varphi_\mathrm{o}$ stays unchanged compared to (7). Due to the tilt of the mirror $\rho$ the angle $\theta_\mathrm{o,b}$ becomes

$$\theta_\mathrm{o,b} = \begin{cases} \pi - 2\rho - \theta_\mathrm{i} & \text{for } \varepsilon = -\pi/4 \\ \pi + 2\rho - \theta_\mathrm{i} & \text{for } \varepsilon = +3\pi/4\,, \end{cases} \tag{11}$$

where the subscript o,b denotes the blazed output direction. From (Instruments, 2008) it is known that the faceted profile creates a $\mathrm{sinc}^2(\cdot)$-envelope on the intensity distribution (10) in each direction. By considering the rotation (1) and applying (3) to (11) to get the blazed parameters $\alpha_\mathrm{o,b}$ and $\beta_\mathrm{o,b}$ one ends up with

$$I(\alpha,\beta) = I_\mathrm{D}(\alpha,\beta)\,\mathrm{sinc}^2\left(\frac{s}{\lambda}(\alpha-\alpha_\mathrm{o,b})\right) \mathrm{sinc}^2\left(\frac{s}{\lambda}(\beta-\beta_\mathrm{o,b})\right)\,, \tag{12}$$

being the complete description of the intensity distribution of the MMA reflected laser beam, where $s$ is the length of an edge of a micromirror.

# 5 OPTIMAL CONDITIONS FOR OPTICAL MIMO COUPLING

Using this equation one can define an optimization program whose result gives the coupling parameters one has to apply in the experimental setup. A simplified program is evaluated as follows:

$$(\theta_{i1}, \varphi_{i1}) = \underset{\substack{0<\theta_{i1}<\pi/2 \\ pi/2<\varphi_{i1}<\pi}}{\arg\max} \; \max_{\substack{\alpha=0 \\ \beta \\ \rho=+\pi/15 \\ \varepsilon=-\pi/4}} I(\alpha, \beta) \, . \tag{13}$$

This program considers the symmetric setup achieved by the DMD rotation by $\varepsilon$. The optimization returns the coupling parameters of the first source i1. Note that $\alpha = 0$ assumes $\theta_o = \pi$. The missing parameters of the second source i2 as well as for the output o are defined by the symmetry.

$$\theta_{i2} = \pi - \theta_{i1} \tag{14}$$

$$\varphi_{i2} = \varphi_{i1} \tag{15}$$

$$\varphi_o = \pi - \varphi_{i1} \tag{16}$$

However, the program (13) is of highly non-convex structure. For a few selected wavelengths the found results were obtained by exhaustive searches over a predefined subset of optimization parameters. The subset is chosen to $61/180 \cdot \pi \leqslant \theta_{i1} \leqslant 71/180 \cdot \pi$ and $0/180 \cdot \pi \leqslant \varphi_{i1} \leqslant 90/180 \cdot \pi$ with steps of $0.025/180 \cdot \pi$ in each direction. The results are given in Tab. 1.

The coupling loss at this point, which is defined by the ratio between the energy located within output direction and its $-3$dB cut-off and the overall energy, for the selected wavelength is $L_{DMD} \approx -1.27$dB. This loss neglects the window attached in front of the MMA, which has to be passed twice, as well as the refelctivity of the mirrors. However, by intuition the angles $\theta_{i1}$ and $\theta_{i2}$ are around $\pi \pm 2\rho$ which is expected by (11) because the output direction is demanded to $\theta_o = \pi$. By presuming this condition to the program (13) an evaluation was made using a wider range of wavelength. To these results regressions on the previously sorted sets were made assuming analytic functions of quadratic form

$$\lambda = f_j(\theta_{i1} = 11/30 \cdot \pi, \varphi_i) = \left[\lambda_m (\varphi_{i1} - \pi/2)^2 + \lambda_o\right] \cdot 10^{-9} \, . \tag{17}$$

The results for the regression parameters $\lambda_m$ and $\lambda_o$ are given in Tab. 2. The family of curves is given in Fig. 3.

With this result one can directly determine optimal coupling parameters for an operating wavelength. The choice, which curve has to be chosen, is a trade off between stability around this operating wavelength, e.g., for wavelength division multiplexing systems, and the mechanical stability of the setup. The flatter the slope of the curve in a chosen working point the more stable is the mechanical setup against variations of the positioning. In contrast, the steeper the curve the higher is the stability for wavelengths around this point.

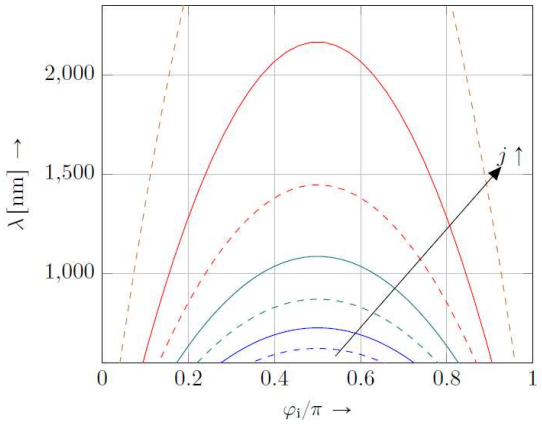


Figure 3: Illustration of Tab. 2.

# 6 REALIZATION AND RESULTS

Fig. 4 shows the first version of the experimental setup. Two collimating lenses ① widen the signal carrying light at the end of two SMFs to two collimated laser beams. These two beams are reflected at the DLP ②, where a previously assigned bit map determines the tilt pattern of the underlying MMA. This consequently decides which source later activates low and which source high order modes, respectively. The camera UI-1240LE ③ measures the reflected laser beam pattern at the main output direction, which will be later replaced by an optic focusing the light pattern onto an attached MMF.

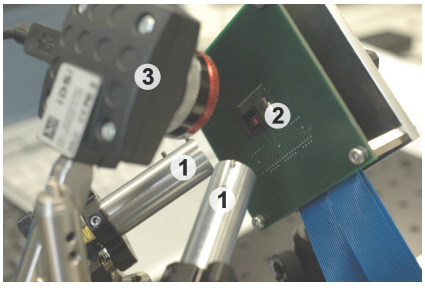


Figure 4: Experimental setup.

The first proof of concept has been made using visible light with wavelength $\lambda = 675$nm. Therefore, the camera gives a more detailed and intuitive insight

Table 1: Optimal coupling parameters of two sources arranged in front of the DLP.

| $\lambda$ | $\varphi_{i1/i2} \cdot 180/\pi$ | $\theta_{i1} \cdot 180/\pi$ | $\theta_{i2} \cdot 180/\pi$ |
|---|---|---|---|
| 675nm | 36.025 | 66.025 | 113.975 |
| 778nm | 44.600 | 65.650 | 114.350 |
| 1326nm | 38.000 | 66.375 | 113.625 |
| 1576nm | 46.125 | 66.000 | 114.000 |

into the mechanical structure and its optimization parameters. The setup has two orthogonal degrees of freedom for each source as previously mentioned: $\theta_{i1/i2}$ and $\varphi_{i1/i2}$. As the experiment is realized using standard optical adjustment components, the parameters, which can be varied, are not orthogonalized to each other. The adjustment becomes an iterative process, which is easier achievable for visible light. The optimized parameters $\varphi_{i1} = \varphi_{i2} \approx 0.62\pi$, $\theta_{i1} \approx 0.37\pi$ and $\theta_{i2} \approx 0.63\pi$ which are chosen from Tab. 2 curve $j = 2$.

The DLP was programmed with a bitmap with an inner circle of ones and zeros around this circle. Hence, one source is seen as a circle on the MMA from the camera, the other one as the corresponding annulus. For the evaluation process the camera took pictures from each source while the parallel source was switched off. Through these pictures a vertical cut was taken to look at the light intensity as a function of the radius. By looking at the orthogonality of the curves generated by the different sources one can conclude to the capability of SDM of this setup. To have a better reference, these curves are compared to light intensity distributions measured at the end surface of a 1.4km MMF. The different distributions are obtained by splices of SMFs to MMFs with centred and offset launching conditions and a subsequent fusion coupler for the mode combining process into that MMF as used in the OMIMO testbed in (Sandmann et al., 2014). Fig. 5 and 6 show the field pattern of the measurements.

Fig. 5 shows the intensity distribution over a vertical cut through a surface of a MMF. The red dashed curve is the distribution produced by a centric splice as described and the blue solid curve produced by an 18$\mu$m eccentric splice. The graph shows well separated low and high order modes as expected. In contrast to Fig. 5, Fig. 6 represents vertical cut through pictures acquired by the camera. For the red dashed curve a centred circle pattern is set to the DLP, for the blue solid curve the corresponding annulus. Note that the parameters $I_{0,1/0,2}$ as well as $r_{0,1/0,2}$ are normalizing constants taken from the measured bit map acquired by different sensors, which only allows a conclusion about relative power distribution within one graph rather than absolute power distribution or a comparison between both graphs with respect to the

Table 2: Analytic functions of shape (17) to obtain optimal coupling parameters using the DLP.

| $j$ | $\lambda_m$[nm] | $\lambda_o$[nm] |
|---|---|---|
| 1 | −311.0 | 624.5 |
| 2 | −354.9 | 728.1 |
| 3 | −415.1 | 872.3 |
| 4 | −507.5 | 1088.0 |
| 5 | −666.7 | 1448.0 |
| 6 | −994.0 | 2167.0 |
| 7 | −1604.0 | 3886.0 |

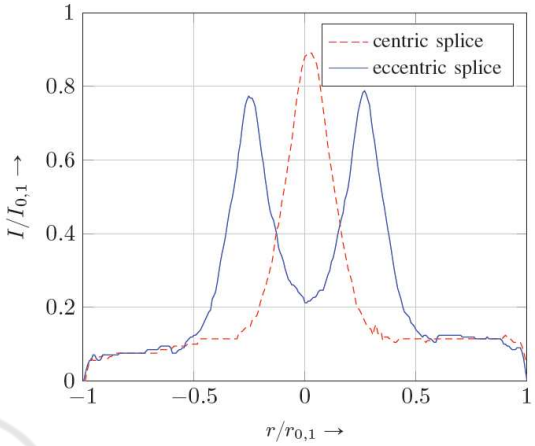


Figure 5: Cut through light intensity measurements: Mode field pattern realized by a fusion coupler with center and offset launch condition.

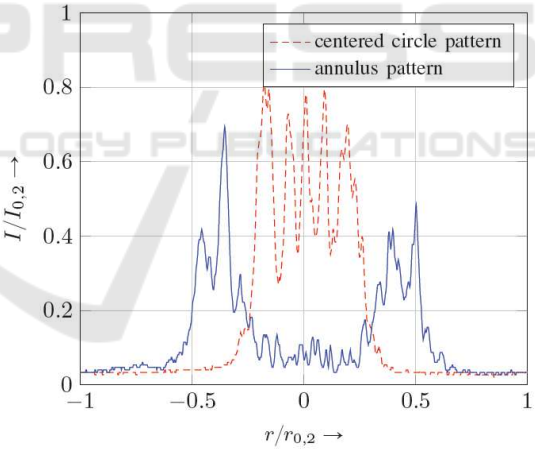


Figure 6: Cut through light intensity measurements: Measured DLP-controlled output pattern.

measured power.

In Fig. 6, the profile is disturbed by fridges. They originate from a non-optimal anti-reflection coating of the protection window attached to the DLP. An additional difficulty appears if one compares the left and right maximum of the annulus which are different in their intensity. The differences is related to the mechanical setup which was not able to match the optimal coupling conditions as described in Sec. 5, perfectly. Nevertheless, a clear separation of both curves can be seen as good as in Fig. 5. This meets the requirement such that the inner source excites low order modes and the outer source high order modes if both sources are concurrently stimulated and the reflected pattern is focused onto a MMF. An advantage of the mode coupling technique utilizing the DLP compared to the splices concatenated with fusion coupler is that the ratio between the inner circle and the outer one can be freely chosen by the tilt pattern of the MMA and is not fixed. Moreover, the achievable theoretical power loss of $L_{\mathrm{DLP}} \approx -1.27\mathrm{dB}$ of our setup is far less than $L_{\mathrm{SLM}} \approx -3\mathrm{dB}$ for a two step serial concatenation of SLMs.

# 7 CONCLUSION

This paper shows how mode group specific excitation in a MMF can be realized using a DMD. The underlying MMA combines two different mode groups simultaneously. Therefore, the DMD features advantages of SLM techniques and fusion couplers while avoiding their specific drawbacks – a controllable mode specific and parallel excitation while having a low insertion loss. Since the MMA is a blazed grating finding the optimal incident angles to the DMD is a complex task. A first proof of the concept is done with visible light. The field pattern of the reflected light of each was captured by a camera to evaluate their orthogonality. Similar to the mode field pattern achieved by offset splices of SMF and MMF the curves of the light intensity distribution generated by different sources are well separated. Hence, the potential of using DMDs for mode selective excitation in a MMF has been demonstrated.

# REFERENCES


Berdagué, S. and Facq, P. (1982). Mode division multiplexing in optical fibers. *Appl. Opt.*, 21(11):1950–1955.

Goodman, J. W. (2005). *Introduction to Fourier Optics*. The McGraw-Hill Companies, Inc., 2nd edition.

Gu, R. Y., Ip, E., Li, M.-J., Huang, Y.-K., and Kahn, J. M. (2013). Experimental demonstration of a spatial light modulator few-mode fiber switch for space-division multiplexing. In *Frontiers in Optics 2013 Postdeadline*. Optical Society of America.

Harvey, J. E. and Vernold, C. L. (1998). Description of diffraction grating behavior in direction cosine space. *Appl. Opt.*, 37(34):8158–8159.

Hayat, G. S. *Handbook of diffraction gratings - ruled and holographic*. JOBIN-YVON S.A.

Hsu, R., Tarighat, A., Shah, A., Sayed, A., and Jalali, B. (2006). Capacity enhancement in coherent optical MIMO (COMIMO) multimode fiber links. *Communications Letters, IEEE*, 10(3):195–197.

Hsu, R. C. J., Shah, A., and Jalali, B. (2004). Coherent optical multiple-input multiple-output communication. *IEICE Electronics Express*, 1(13):392–397.

Instruments, T. (2008). Using lasers with DLP DMD technology. Technical report, Texas Instruments.

Ryf, R., Fontaine, N. K., Mestre, M. A., Randel, S., Palou, X., Bolle, C., Gnauck, A. H., Chandrasekhar, S., Liu, X., Guan, B., Essiambre, R.-J., Winzer, P. J., Leon-Saval, S., Bland-Hawthorn, J., Delbue, R., Pupalaikis, P., Sureka, A., Sun, Y., Grüner-Nielsen, L., Jensen, R. V., and Lingle, R. (2012). $12 \times 12$ MIMO transmission over 130-km few-mode fiber. In *Frontiers in Optics 2012/Laser Science XXVIII*, page FW6C.4. Optical Society of America.

Sandmann, A., Ahrens, A., and Lochmann, S. (2014). Experimental description of multimode mimo channels utilizing optical couplers. In *Photonic Networks; 15. ITG Symposium; Proceedings of*, pages 1–6.

Schollmann, S., Schrammar, N., and Rosenkranz, W. (2008). Experimental realisation of $3 \times 3$ MIMO system with mode group diversity multiplexing limited by modal noise. In *Optical Fiber communication/-National Fiber Optic Engineers Conference, 2008. OFC/NFOEC 2008. Conference on*, pages 1–3.

Shah, A., Hsu, R., Tarighat, A., Sayed, A., and Jalali, B. (2005). Coherent optical MIMO (COMIMO). *Lightwave Technology, Journal of*, 23(8):2410–2419.

Tang, K.-T. (2007). *Mathematical Methods for Engineers and Scientists 2*. Springer-Verlag Berlin.

Yoder, L. A., Duncan, W. M., Koontz, E. M., So, J., Bartlett, T. A., Lee, B. L., Sawyers, B. D., Powell, D., and Rancuret, P. (2001). DLP technolgy: applications in optical networking. In *SPI Proceedings*, volume 4457, pages 54–61.